Comparison of rheological parameters of asphalt binders obtained from bending beam rheometer and dynamic shear rheometer at low temperatures

Jean-Claude Carret, Augusto Cannone Falchetto, Mihai Marasteanu, Hervé Di Benedetto, Michael Wistuba, Cédric Sauzeat

Comparison of rheological parameters of asphalt binders obtained from bending beam rheometer and dynamic shear rheometer at low temperatures

Jean-Claude Carret[a], Augusto Cannone Falchetto[b*], Mihai O. Marasteanu[c], Hervé Di Benedetto[a], Michael P. Wistuba[b] and Cedric Sauzeat[a]

[a]ENTPE, Laboratory LGCB & LTDS (UMR CNRS), University of Lyon, Lyon, Rue M. Audin, 69518, Vaulx en Velin, France
[b]Technische Universität Braunschweig, ISBS, Beethovenstraße 51b, 38106 Braun-schweig, Germany
[c]Department of Civil, Environmental, and Geo- Engineering, University of Minnesota, Minneapolis, MN 55455–0116, USA

In this paper, an investigation was performed to determine if the complex modulus obtained from frequency sweeps performed with the dynamic shear rheometer (DSR) can be used to accurately predict the creep compliance obtained experimentally using the bending beam rheometer (BBR). Two sets of asphalt binders were tested at low, intermediate, and high temperatures and the results were analysed using 2S2P1D and DBN rheological models. DSR and BBR testing was performed in two different laboratories using different equipment manufacturers. It was found that significant differences are observed between the creep stiffness obtained with DSR and BBR devices, most likely due to the different preparation and conditioning of the test specimens in different cooling media.

Keywords: asphalt binder; linear viscoelasticity; dynamic shear rheometer (DSR); bending beam rheometer (BBR); creep compliance; physical hardening

1. Introduction

One of the most significant achievements in the area of paving asphalt materials characterisation was the development of the Strategic Highway Research Program (SHRP) performance grade (PG) specifications at the beginning of the 1990s. The PG tests and analyses, detailed in a number of American Association of State Highway and Transportation Officials (AASHTO) specifications (AASHTO M320, 2010; AASHTO T313, 2012; AASHTO T315, 2012), are used to specify the asphalt binders used in pavement applications and also serve as primary tools to investigate the behaviour of asphalt binders in many research studies. The success of the PG system can be attributed, on one hand, to the innovative application of fundamental concepts to asphalt binder material characterisation and, on the other hand, to the reasonable level of complexity of the test methods and analyses required as part of these specifications.

Most of the data required to determine the PG of a binder are obtained from two experimental testing procedures: frequency sweeps performed with a dynamic shear rheometer (DSR) (AASHTO T315, 2012) at high and intermediate temperatures, and bending creep tests performed with a bending beam rheometer (BBR) (AASHTO T313, 2012) at low temperatures. The parameters obtained in DSR are: $|G^*(\omega)|$ that represents the absolute value of the shear complex

*Corresponding author. Email: a.cannone-falchetto@tu-bs.de

modulus, and $\delta(\omega)$ that represents the corresponding phase angle. The parameters obtained from BBR are: $S(t)$ that represents the creep stiffness (inverse of creep compliance), and m-value that represents the absolute value of the slope of the creep stiffness versus time curve on a double logarithmic scale.

Preparing BBR beams for testing requires approximately 15 g of binder per beam, while the DSR test requires only a few grams. As low-temperature tests are performed on pressure aging vessel (PAV)-aged binders or binders recovered from field cores, which are difficult to obtain in large quantities, it becomes important to explore the possibility of replacing the BBR test with the DSR test that requires much smaller quantities of materials. A number of researchers have explored this possibility (Claudy, Letoffe, King, & Plancke, 1992) and recently Farrar, Sui, Salmans, and Qin (2013) proposed a new DSR geometry and inter-conversion methods to obtain creep stiffness and m-values from DSR tests at low temperature. According to the theory of viscoelasticity (Ferry, 1980), any linear viscoelastic (LVE) function can, in theory, be converted into any other viscoelastic function.

2. Objective

In this paper, an investigation was performed to determine if the complex modulus obtained from DSR testing can indeed be used to accurately predict the creep compliance obtained using BBR testing. As the two BBR parameters S(60s) and m(60s) are used to obtain the lower limit of the binder PG, it becomes critical to determine if DSR testing and LVE inter-conversions match the BBR results at the same temperature. The investigation was prompted by the fact that physical hardening, that significantly affects BBR results, has been well documented during SHRP research effort and received considerable attention over the years, while this effect has not been studied for DSR testing, mostly because of testing equipment limitations at low temperatures. It is also worth mentioning that DSR testing is performed in air, while BBR creep tests are performed in ethanol.

3. Materials and testing

Two sets of materials were used in this study. The first set was tested as part of a previous investigation (Marasteanu & Anderson, 2000) and the second set represents asphalt binders recently tested in Germany.

The first set consists of four of the SHRP core asphalt binders. The binders were selected based on their asphaltene content (AC) and crystallised fraction (CF), which are known to influence physical-hardening effects: AAD1 has low CF and high AC; AAF1 has high CF and high AC; AAG1 has low CF and low AC; and AAM1 has high CF and low AC. All samples were tested in the unaged condition.

DSR frequency sweep data were obtained using three types of geometries: 25, 8 mm, and torsion bar. For the torsion bar geometry, a laboratory procedure described elsewhere (Marasteanu & Anderson, 2000) was used. To minimise potential nonlinear effects, the strain was changed with each decade change in frequency. All tests were performed in air. BBR creep tests were performed in ethanol at three consecutive specification temperatures according to the asphalt binder PG (low PG + 4°C, low PG + 10°C and low PG + 16°C) as listed in Table 1. The three temperatures were chosen so that the deflection values obtained were within the BBR test specification limits (from 0.08 to 4.00 mm). A summary is given in Table 1. All tests were replicated twice.

Table 1. Summary of testing protocol.

DSR
• Frequency sweeps as follows: (i) Parallel plate geometry (1 mm-height × 25 mm-diameter): 46°C, 52°C, 58°C, 64°C, 70°C and 76°C (ii) Parallel plate geometry (1 mm-height × 8 mm-diameter): 4°C, 10°C, 16°C, 22°C, 28°C, 25°C, 34°C and 40°C (iii) Torsion bar geometry (3.3 mm-thick × 12.7 mm-wide × 38.1 mm-long): –30°C, –24°C, –18°C, –12°C, –6°C and 0°C. Conditioning time varied from 30 min to 2 h
BBR
• 4 min creep with 100 g load followed by 4 min of recovery at three temperatures in the rage − 30°C, − 24°C, − 18°C, − 12°C and − 6°C, depending on asphalt binder low PG. Conditioning times varied from 1 to 48 h • 4-minute creep with 50, 100 and 150 g load, respectively, at the intermediate of the three temperatures. Conditioning time was 1 h

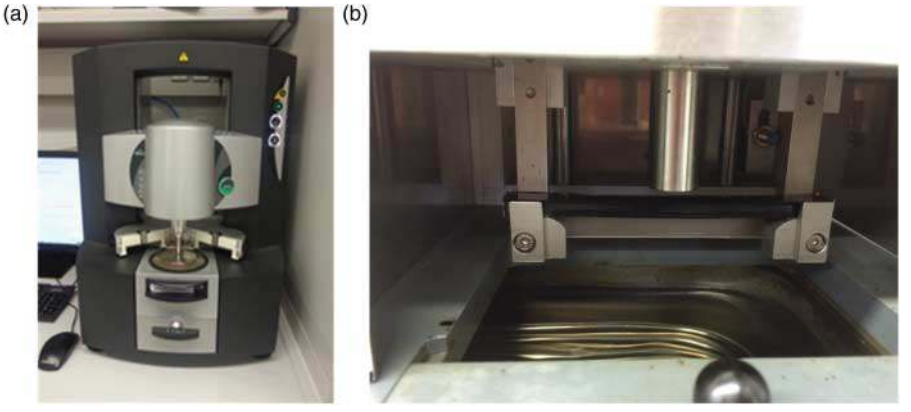

Figure 1. (a) DSR testing device, (b) BBR testing device.

The second set consists of two asphalt binders tested in the unaged condition at the Pavement Engineering Centre at the Technische Universität Braunschweig. The first asphalt binder is a plain binder having a 50/70 penetration window (EN 1426, 2007), hereafter identified as AB 50-70, while the second is a 45/80-65 polymer-modified binder with a penetration range of 45/80 (EN 1426, 2007) and a softening temperature of 65°C (EN 1427, 2007), named AB 45-80-65.

DSR frequency sweep data were obtained according to current specifications (AASHTO T315-12, 2012; EN 14770, 2012) using two different plate sizes: 8 mm plates were used for temperatures between 0°C and 40°C (0°C, 4°C, 10°C, 16°C, 22°C, 28°C, 34°C and 40°C), while 4 mm plates were needed for lower temperatures down to − 40°C (− 40°C, − 36°C, − 30°C, − 24°C, − 18°C, − 12°C, − 6°C, 0°C, 4°C and 10°C). For both geometries, tests were performed starting from the lowest temperature and allowing an equilibrium time of 30 min before the actual test at the specific temperature. Specimens were initially conditioned for 1.5 h at the lowest temperature corresponding to − 40°C and 0°C, for the two geometries, respectively. Conditioning and testing were performed using air as the cooling medium. The range of frequencies was selected between 0.01 and 10 Hz and the lowest frequency was imposed as the initial frequency for all temperatures. Figure 1 shows the DSR device for asphalt binder together with the two testing geometries.

BBR creep tests were performed according to AASHTO and EN (European Norm) specifications (AASHTO T313-12, 2012; EN 14771, 2012). Conditioning (1 h) and testing were performed using ethanol as the cooling medium. The same two testing temperatures were selected for both asphalt binders: -24°C and -18°C. These two temperatures were also used for DSR testing and, therefore, provide the possibility of a direct comparison of the experimental data obtained from oscillatory and static loading without the potential errors that may be associated with time–temperature superposition shifting. Figure 1 presents the DSR and BBR equipments used in the laboratory at Braunschweig.

4. Tools to analyse DSR rheological data

When performing simple or complex analyses on sets of rheological data obtained over a wide range of temperatures, it is good practice to first examine the data in a graphical form. Asphalt binders do not exhibit sudden changes in their behaviour with respect to time or temperature. Therefore, any discontinuities in the test data or any sudden change in the slope of the curves when changing test temperatures or loading time or frequency can most likely be attributed to testing error.

Plots of $|G^*|$ and of phase angle versus frequency at different temperatures are very useful for identifying errors. However, when multiple test temperatures are used, two other graphical representations can be used.

The first one is the Cole–Cole plot that is a graphical representations of the two components of the complex modulus, G' (horizontal axis) and G'' (vertical axis), when complex modulus is expressed as $G^* = G' + \mathrm{i}\, G''$. An example is shown in Figure 2 for asphalt binder AAD1.

One advantage of this representation is that it can detect small errors in the data since both axes have normal scales. However, one big disadvantage of using the normal numerical scale is the fact that only test data at temperatures below zero are visible in this plot, while the test data above zero are basically invisible, as clearly seen from Figure 2. It should also be mentioned that the peak observed for G'' is associated with the glass transition temperature (Anderson & Marasteanu, 1999; Anderson, Marasteanu, & Liu, 1999).

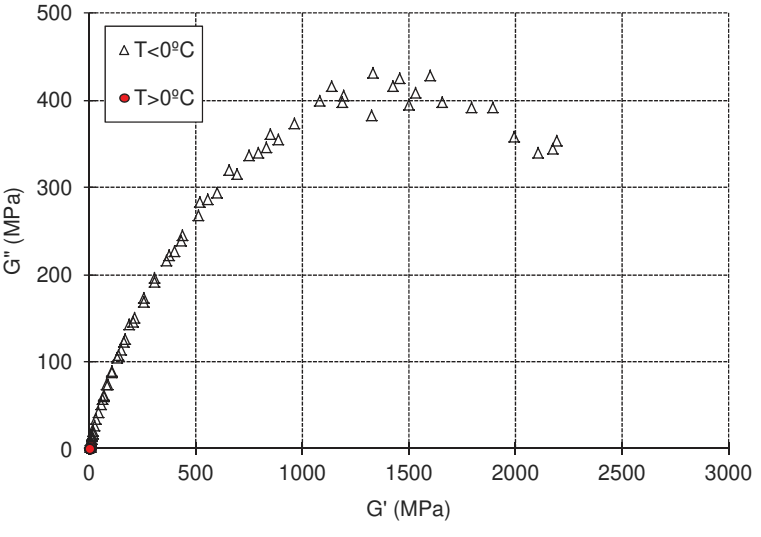

Figure 2. Cole–Cole plot for asphalt binder AAD1.

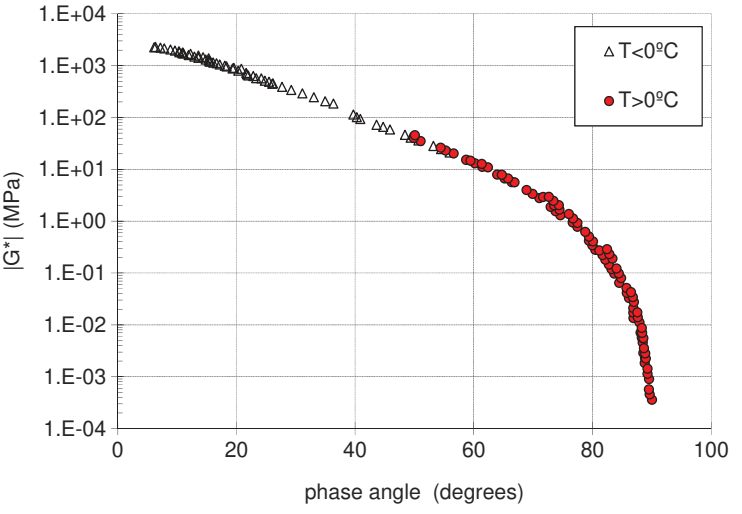

Figure 3. Black space plot for asphalt binder AAF1.

One simple way to avoid this problem is using the Black diagram, which uses the two components of the complex modulus, $|G^*|$ and phase angle δ, when the complex modulus is expressed as $G^* = |G^*|e^{i\delta}$. In this representation, the vertical axis is log $|G^*|$ and the horizontal axis is the phase angle on the normal scale. While the log scale makes the identification of small errors less obvious, it allows for visible representation of the entire temperature range of testing. If the material is linear, thermo-rheologically simple, and there are no testing errors, a smooth curve is obtained. An example is shown in Figure 3 for asphalt binder AAF1.

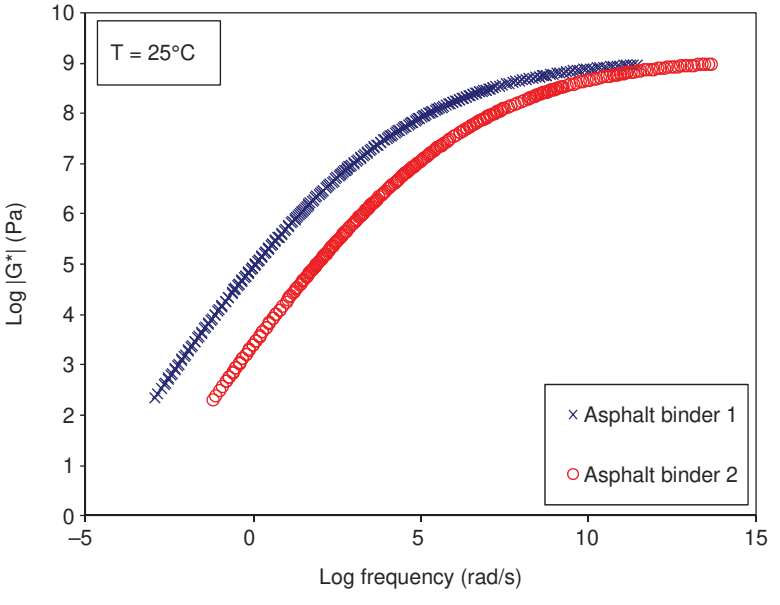

Figure 4. Temperature dependency of two asphalt binders having similar master curves shapes.

Cole–Cole and Black space representations do not require any shifting for data generated at different temperatures. While this is a big advantage, it also makes it impossible to detect errors in temperature measurement and does not provide any information on the temperature dependency of the material. For example, two asphalt binders may have similar master curves shapes but different temperature dependencies, as shown in Figure 4. Neither Cole–Cole nor Black space will detect any difference between the two binders.

A full representation of the material behaviour can be obtained through the use of master curves that are based on rheological models. These models can describe both the frequency (time) and temperature dependency of the material and some of the models can be used to obtain other viscoelastic functions, such as creep and relaxation modulus, from frequency sweep experiments. This latter approach is used in this investigation to compare DSR and BBR results at low temperature.

5. Rheological models

Two complementary models, developed at the Ecole Nationale des Travaux Publics de l'Etat (ENTPE) laboratory, were used in the analysis of the DSR data:

- The LVE with the continuous spectrum 2S2P1D (two springs, two parabolic elements and one dashpot) model introduced by Di Benedetto, Olard, Sauzéat, and Delaporte (2004) and Olard and Di Benedetto (2003) characterises the behaviour of bituminous materials in the linear domain (i.e. for small strain amplitudes);
- The viscoplastic DBN (Di Benedetto, Neifar) model (Di Benedetto, Neifar, Sauzéat, & Olard, 2007; Di Benedetto & Olard, 2009; Neifar & Di Benedetto, 2001; Olard & Di Benedetto, 2005) predicts the general thermo-viscoelastoplastic behaviour of bituminous materials.

5.1. *2S2P1D model*

The 2S2P1D (two springs, two parabolic creep elements, one dashpot) is a generalisation of the Huet model (Huet, 1963). The Huet model has an analytical creep function (Cannone Falchetto, Marasteanu, & Di Benedetto, 2011; Moon, Cannone Falchetto, & Marasteanu, 2013) but does not simulate correctly asphalt materials behaviour on the whole frequency and temperature range, especially at high temperature and/or low frequency. The 2S2P1D model is based on a simple combination of physical elements (springs, parabolic creep element, and dashpot) as shown on its analogical representation in Figure 5. This model can also simulate the three-dimensional behaviour of bituminous mixtures, binders, or mastics (Di Benedetto, Delaporte, & Sauzéat, 2007; Di Benedetto et al., 2004). Calibration of the 2S2P1D model is obtained from an optimisation using experimental data.

At a given temperature, complex modulus of the 2S2P1D model is given by Equation (1)

$$E^*_{2S2P1D}(\omega) = E_{00} + \frac{E_0 - E_{00}}{1 + \delta(\mathrm{j}\omega\tau)^{-k} + (\mathrm{j}\omega\tau)^{-h} + (\mathrm{j}\omega\beta\tau)^{-1}}, \quad (1)$$

where j is the complex number defined by $\mathrm{j}^2 = -1$; ω is the angular frequency, $\omega = 2\pi f$, where f is the frequency; k, h constants such as $0 < k < h < 1$; δ constant; E_{00} is the static modulus when ω tends towards 0, for asphalt it is equal to 0; E_0 is the glassy modulus when ω tends towards$+\infty$; η the Newtonian viscosity of the dashpot, $\eta = (E_0 - E_{00})\,\beta\tau$ and τ the characteristic time, whose value varies only with temperature.

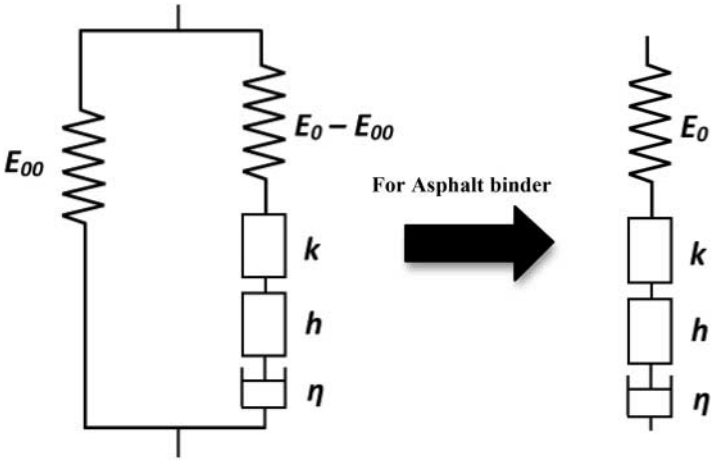

Figure 5. Analogical representation of the 2S2P1D model: general case (left), for asphalt (right).

The time–temperature superposition principle is verified in linear and non-linear domains (Nguyen, Pouget, Di Benedetto, & Sauzéat, 2009; Nguyen, Sauzéat, Di Benedetto, & Tapsoba, 2013; Nguyen, Di Benedetto, Sauzéat, & Tapsoba, 2013) using:

$$\tau(T) = a_T(T)\tau_0, \tag{2}$$

where a_T is the shift factor at the temperature T given by: the WLF (Williams–Landel–Ferry) (Ferry, 1980) equation (Equation (3))

$$\log(a_T) = -\frac{C_1(T - T_r)}{C_2 + T - T_r}. \tag{3}$$

C_1 and C_2 represent the two WLF constants and T_r the reference temperature. At a given temperature, six constants ($E_0,\ \delta,\ k\ ,h,\ \beta,\ \tau_0$) are required to model the LVE properties of asphalts on the whole range of frequencies. When temperature effects are considered, eight constants are needed, including the two WLF constants ($C_1,\ C_2$).

5.2. *DBN model*

Research performed at ENTPE led to the development of the DBN model which is an attempt to describe with one formulation the different types of behaviour observed for bituminous mixtures. This model is also able to simulate the behaviour for any bituminous materials such as binders, mastics, and mixes. Only the main aspects of the DBN model are presented in this paper. More details can be found elsewhere (Di Benedetto, Neifar et al., 2007; Di Benedetto & Olard, 2009; Neifar & Di Benedetto, 2001; Olard & Di Benedetto, 2005).

The 1D representation of the DBN model is composed of one spring (modulus E_0) and n elementary bodies (each of them composed by an elastoplastic (i.e. non viscous) body (EP) in parallel with a dashpot (linear V body) as shown in Figure 6. The number of elementary bodies (n) can be chosen arbitrarily as the calibration procedure always needs the same number of constants (the constants from the 2S2P1D model and plastic functions not introduced in this paper). If n is high, simulation becomes closer to the experimental data. In the LVE domain (i.e. for small strain amplitude domain) EP bodies become springs of rigidity E_i, and the DBN model becomes a Generalised Kelvin Voigt (GKV) model (Figure 6). In that case, calibration of the

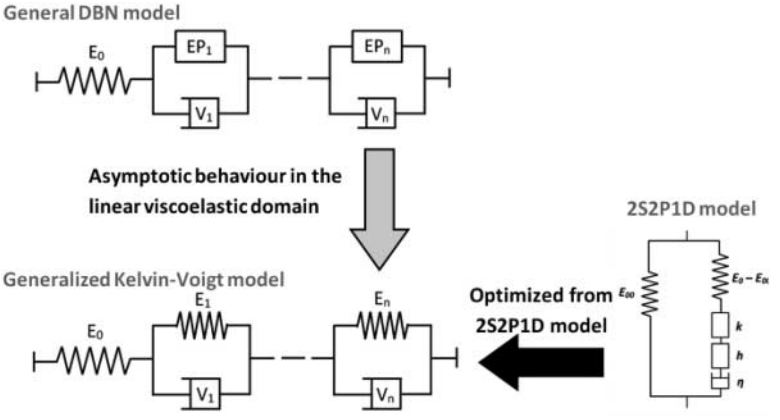

Figure 6. Analogical 1D representation of the DBN model, which corresponds to the GKV model in the LVE domain (small strain amplitude).

n elementary bodies is made from parameters of the 2S2P1D model (also developed at LGCB-ENTPE and presented in the previous section). 2S2P1D is a continuous spectrum model with a limited number of constants (nine in the mono-dimensional case). When increasing number *n* of elementary bodies, the difference between the optimised DBN model and 2S2P1D model decreases on the whole temperature–frequency range. Theoretically, this difference becomes nil for *n* equal to infinity. In this paper, the number of considered elementary bodies is $n = 90$, and $E_{00} = E_n = 0$ since only asphalt binders were considered. Figure 7 shows that $n = 90$ gives quite a good approximation of 2S2P1D on the whole temperature–frequency range. Due to lack of space, readers are invited to read given references on LGCB-ENTPE work, for more details on the general procedure.

5.3. *Methodology used in this paper*

For each tested asphalt binder, data from DSR experiments are fitted using the 2S2P1D model. As the DSR device gives complex shear modulus (G^*), the experimental data are multiplied by 3 to obtain complex modulus (E^*) ($E^* = 3G^*$). To apply coefficient "3", an isotropic behaviour and Poisson's ratio of 0.5 are assumed. This last hypothesis, made to simplify the analysis, could be improved if three-dimensional expression of 2S2P1D is considered (Di Benedetto, Delaporte et al., 2007; Tiouajni, Di Benedetto, Sauzéat, & Pouget, 2011). The 2S2P1D model fitting was presented in several papers from the ENTPE team, for different types of bituminous materials (Baaj, Ech, Tapsoba, Sauzéat, & Di Benedetto, 2013; Delaporte, Di Benedetto, Chaverot, & Gauthier, 2009; Di Benedetto, Sauzéat, & Sohm, 2009; Mangiafico et al., 2013, 2014; Mounier, Di Benedetto, & Sauzéat, 2012; Pouget, Sauzéat, Di Benedetto, & Olard, 2010a, 2010ab, 2012; Tapsoba, Sauzéat, Di Benedetto, Baaj, & Ech, 2014). The number of analysed cycles should be correctly chosen to avoid biased effects, such as heating and thixotropy as shown elsewhere (Di Benedetto, Nguyen, & Sauzéat, 2011; Nguyen, Di Benedetto, & Sauzéat, 2012).

The list of 2S2P1D constants for the two sets of tested asphalt binders presented in this paper is given in Table 2.

Then, the GKV model (asymptotic expression of DBN model) having 90 elements is optimised from the calibrated 2S2P1D model for each material. The optimisation process is explained in Tiouajni et al. (2011). The process is quite simple as it is made by an excel sheet developed at ENTPE Laboratory. The GKV model simulation with 90 elements gives a quite similar result

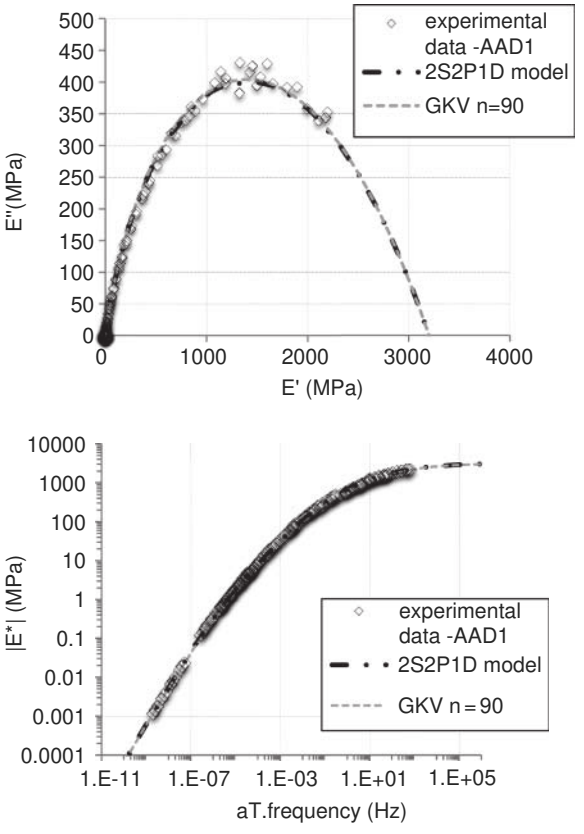

Figure 7. Experimental results of the complex modulus test on binder AAD1 with 2S2P1D and the GKV model (90 elements): simulation plotted for the complex Young's modulus E^*. Above: Cole–Cole diagram; below: mastercurve at − 18°C diagram.

Table 2. 2S2P1D constants for tested asphalt (E^* modulus from DSR data).

Parameters	E_0 (MPa)	δ	k	h	β	$\tau_{-18°C}$ (s)	C_1	C_2
AAD1	3200	2.7	0.28	0.62	220	0.15	26.87	135.22
AAF1	3100	2.6	0.25	0.52	170	6	25.06	107.62
AAM1	2300	3.8	0.27	0.58	200	12	24.57	99.96
AAG1	2900	2.1	0.26	0.52	30	140	18.02	56.52
AB 50–70	1850	2.2	0.20	0.53	120	35	5.4E7	3.2E8
AB 45–60–80	1400	6	0.23	0.57	450	15	1.5E6	9.8E6

than the 2S2P1D model as seen in Figure 7 where an example of 2S2P1D fitting is presented for asphalt binder AAD1.

From values η_i and E_i of the GKV model it is quite easy to write the creep function ($F_{\text{simul DSR}(t)}$) for simple tension and compression loading (compliance). This creep function is given in Equation (4)

$$F_{\text{simul DSR}(t)} = \frac{1}{E_0} + \sum_{i=1}^{n-1} \frac{1}{E_i}(1 - e^{-t/\tau_i}) + \frac{1}{\eta_n}. \tag{4}$$

The inverse of $F_{\text{simul DSR}(t)}$ gives the creep stiffness function $S_{\text{simul DSR}(t)}$ (Equation (5)), which is compared with BBR creep stiffness data, $S(t)$, in the next sections, for the different asphalts

$$S_{\text{simul DSR}(t)} = \frac{1}{F_{\text{simul DSR}(t)}}. \tag{5}$$

6. Comparison of DSR and BBR data

The procedure described above was used to convert DSR frequency sweep data to BBR creep stiffness (inverse of creep compliance). To eliminate any errors associated with the applicability of the time–temperature superposition principle, the comparisons were performed at the same test temperatures. Since Poisson's ratio is not commonly determined for asphalt binders, a constant value of 0.5 was assumed for all conversions from shear to tension to simplify the analysis, as explained in the previous section.

Typical plots of the data obtained for the two sets of asphalt binders are shown in Figures 8 and 9.

Visual inspection of all the plots prepared for the four core asphalt binders at three different test temperatures showed that in all cases the measured BBR creep stiffness was larger than the creep stiffness calculated from DSR data. The largest differences were observed for asphalt binders AAD1 and AAF1. The smallest differences were observed for asphalt binder AAG1.

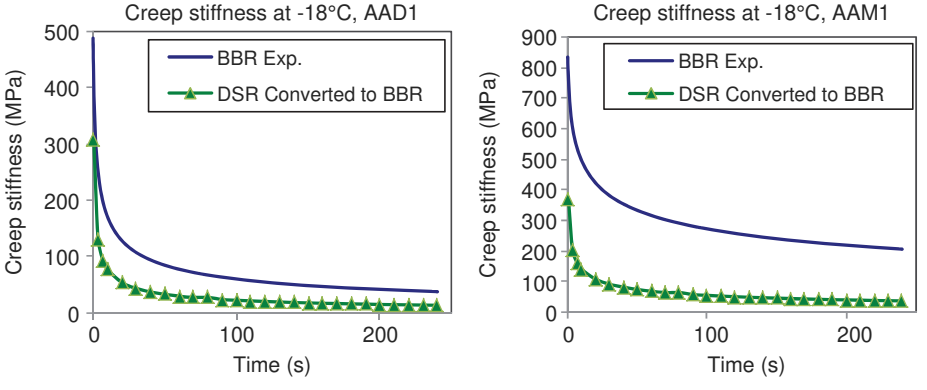

Figure 8. Comparison of DSR and BBR data for two of the core asphalt binders at − 18°C.

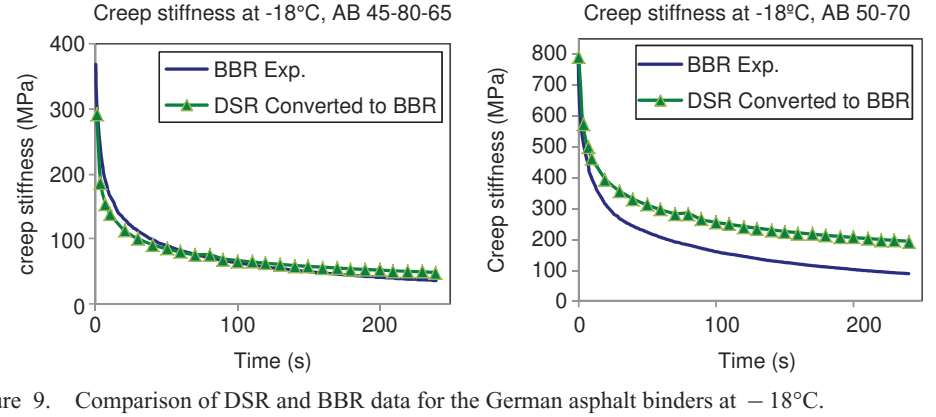

Figure 9. Comparison of DSR and BBR data for the German asphalt binders at − 18°C.

Reducing Poisson's ratio values did not improve the match. A Poisson ratio of 0.3 results in a multiplication factor of 2.6 instead of 3, a drop of only 13% that cannot explain differences more than double observed for some of the binders. A less clear trend is observed for the two German asphalt binders. For binder AB 45-80-65, the DSR and BBR almost match while for binder AB 50-70 the opposite of what was observed for the core binders is noticed.

It can also be observed that using vertical shifting does not provide a good matching between the BBR experimental results and the creep stiffness curves obtained from the conversion of the DSR data. A horizontal shift on the time scale appears to be a better alternative, similar

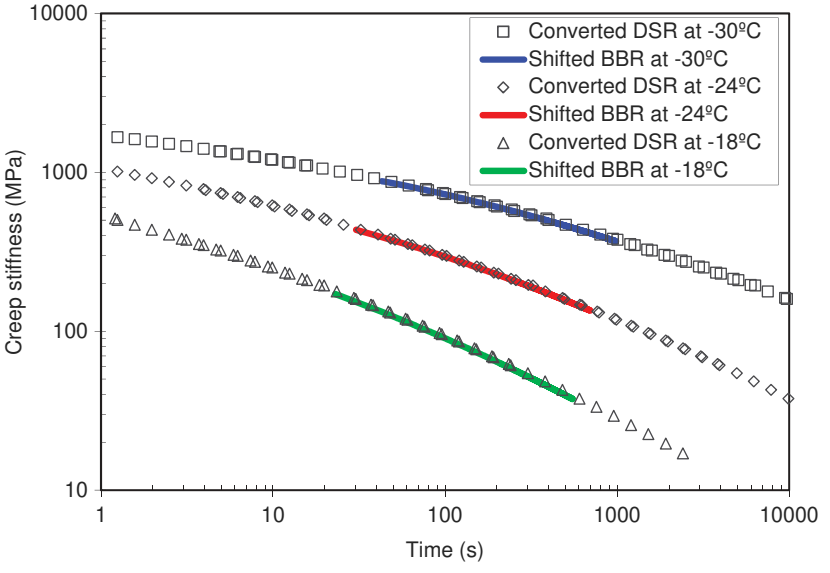

Figure 10. Creep stiffness for AAD1, shifted BBR and converted DSR data.

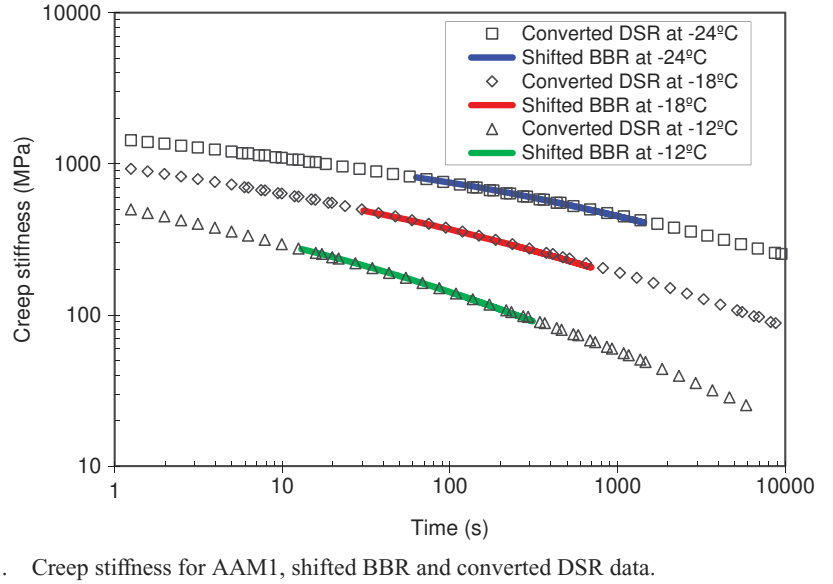

Figure 11. Creep stiffness for AAM1, shifted BBR and converted DSR data.

to the trend observed in the BBR physical-hardening data; in a previous paper (Anderson & Marasteanu, 1999) it was shown that the effect of physical hardening on BBR stiffness could be approximated with a shift to a higher test temperature, which translates to a shift on the time axis. This approach was also used with the binders used in this study and it was found out that horizontal shifting of the BBR creep compliance results in an almost perfect match of the converted DSR data. The shifting factors for asphalt binder AAD1 were 2.3, 2.9 and 4.1 for temperature −18°C, −24°C and −30°C, respectively. In the case of asphalt binder AAM1 the following shifting factors were used: 1.3, 2.9 and 6.0 corresponding to temperatures −12°C, −18°C and −24°C. Examples are shown in Figures 10 and 11. The logarithmic scale was used to show all three temperatures.

It is therefore plausible to explain the difference between the BBR data and the converted DSR data as the result of a difference in physical-hardening effects on the two samples. A limited experiment was performed on the four SHRP core asphalt binders to investigate this issue.

7. Physical-hardening effects

Physical hardening of asphalt binders tested at low temperatures has been well documented during SHRP (Anderson et al., 1994; Bahia, 1991). However, these conclusions were based entirely on BBR data. No studies have been reported on physical-hardening effects for the DSR at low

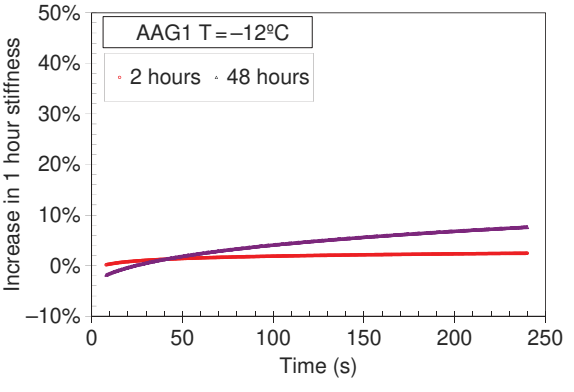

Figure 12. Change in creep stiffness for AAG1 due to physical hardening.

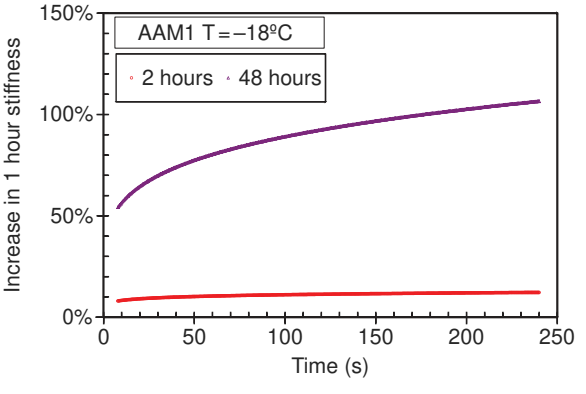

Figure 13. Change in creep stiffness for AAM1 due to physical hardening.

temperatures. For this reason, the asphalts used in this study were tested after varying conditioning times to identify the effects of physical ageing for both DSR and BBR conditions. Due to the difficulties associated with longer conditioning times for DSR, conditioning time was limited to a maximum of 2 h. For BBR, individual samples were tested at each test temperature after 1, 2, 24, and 48 h conditioning times.

No significant differences in complex modulus (absolute value) or phase angle were observed in DSR torsion bar tests for the various conditioning times for any of the four asphalt binders; the differences observed were less than the testing errors associated with the test results obtained.

As expected, physical hardening did play a significant role in the BBR tests. The magnitude of the effect was loading time dependent and asphalt binder dependent. The change in stiffness and *m*-value increases with the increase in loading time. Asphalt AAG1, characterised by low asphaltene and wax content, showed an increase in stiffness after 48 h of isothermal cooling to be between 0% and almost 10% (Figure 12). For AAD1, with high AC and low wax content, the increase in stiffness after 48 h ranged from 35% to 60%, while for AAM1 that has high wax content, ranged from 60% to 110% (Figure 13).

8. Cooling medium effects

Other factors may be responsible for the differences observed when comparing DSR and BBR data. One possible factor is the cooling medium: the DSR uses refrigerated air, while the BBR

Table 3. Asphalt binder details and experimental design.

Binder	Ageing	Cooling media	Conditioning time
Citgo PG58-28 plain	RTFOT – PAV (control)	E (control) – PA – Air	1 h (control)–20 h
MIF PG58-34 Elvaloy	RTFOT – PAV (control)	E (control) – PA – Air	1 h (control)–20 h
Marathon PG58-28 plain	RTFOT – PAV (control)	E (control) – PA – Air	1 h (control)
Valero PG58-28 plain (control)	RTFOT – PAV (control)	E (control) – PA – Air	1 h (control)

Note: RTFOT, rolling thin film oven test.

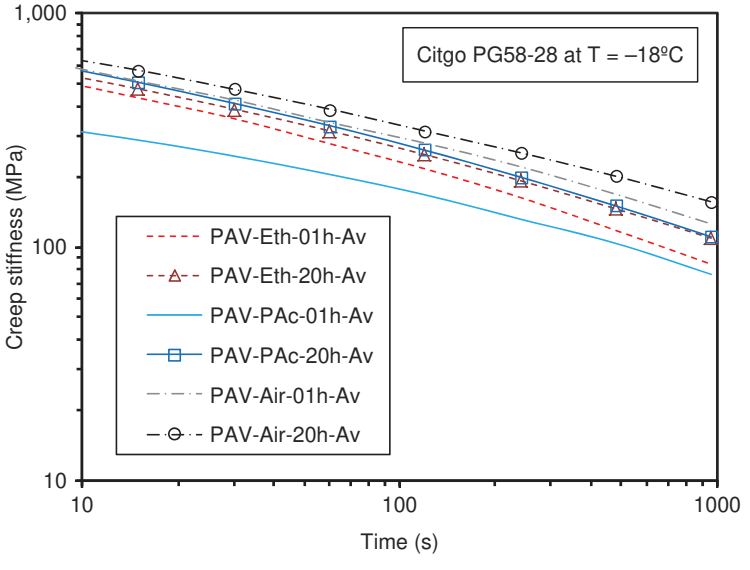

Figure 14. BBR creep stiffness curves for Citgo PG58-28.

uses ethanol to condition the sample. This difference may result in different cooling rates in the DSR and BBR samples. In addition, ethanol has been shown to interact with the asphalt binder and significantly affect strength properties of the binders (Cannone Falchetto, Marasteanu, Balmurugan, & Negulescu, 2014; Marasteanu, Cannone Falchetto, Turos, & Le, 2012).

A simple study, performed as part of a different investigation, brings support to this hypothesis. Four asphalt binders were tested using BBR at one single testing temperature corresponding to 10°C above the lower limit of the performance (PG) of the binders. The tests were performed in three cooling media: ethanol (E), potassium acetate (PA) typically used in binder direct tension testing, and air. For two of the binders, two conditioning times were also used: 1 and 20 h. Table 3 presents materials details and experimental design.

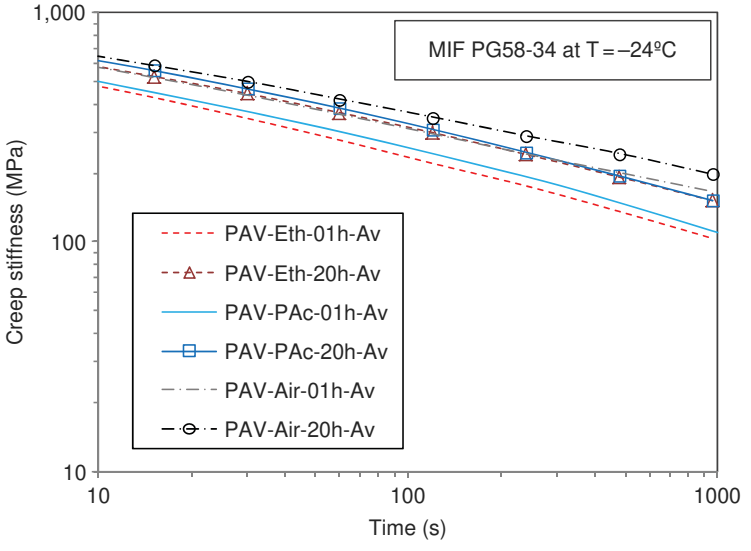

Figure 15. BBR creep stiffness curves for MIF PG58-34.

Table 4. ANOVA *F* tests results of asphalt binder for (a) *S*(60) and (b) *m*(60).

Source – *S*(60s)	*F*	*p*-Value
(a)		
Binder type	489.6	1E – 08
Cooling medium	114.7	1E – 08
Conditioning time	92.9	1E – 08
Ageing	338.8	1E – 08
Cooling medium.ageing	4.8	.011
Source – *m*(60s)	*F*	*p*-value
(b)		
Binder type	123.9	1E – 08
Cooling medium	242.7	1E – 08
Conditioning time	136.8	1E – 08
Ageing	836.7	1E – 08
Conditioning time.cooling medium	3.8	.029

Figures 14 and 15 show the average (Av) creep stiffness curves for Citgo and MIF asphalt binders, and Table 4(a) and 4(b) presents the results of the statistical analysis (ANOVA) for creep stiffness and m-value at $t = 60$s: $S(60)$ and $m(60)$.

These results follow the same trend observed in the previous section: the measured BBR creep stiffness (in ethanol) was less than the creep stiffness calculated from DSR data (in air). It also indicates that the changes are binder specific, which makes this problem more complex.

9. Conclusions

Based on the materials, laboratory equipment, testing protocols, and analyses used in this study, it was found that significant differences are observed between the creep stiffness obtained with DSR and BBR devices. The most probable factor responsible for these differences is the different cooling media used in the two instruments that may result in different cooling rates as part of the preparation and conditioning of the samples (DSR – air, BBR – ethanol fluid) and, therefore, in different physical-hardening effects. The observations and findings from this study do not render the viscoelastic properties measured in the DSR and BBR invalid. They demonstrate, however, that there are other factors associated with their measurement that makes a direct comparison, based strictly on LVE concepts, inaccurate. Therefore, replacing the current BBR specification with a similar specification based on DSR experimental data cannot be successful until these issues are addressed.

Disclosure statement

No potential conflict of interest was reported by the authors.

References

AASHTO M320-10-UL. (2010). *Standard specification for performance-graded asphalt binder*. Washington, DC: Author.

AASHTO T313-12-UL. (2012). *Standard method of test for determining the flexural creep stiffness of asphalt binder using the bending beam rheometer (BBR)*. Washington, DC: Author.

AASHTO T315-12-UL. (2012). *Standard method of test for determining the rheological properties of asphalt binder using a dynamic shear rheometer (DSR)*. Washington, DC: Author.

Anderson, D. A., Christensen, D. W., Bahia, H. U., Dongre, R., Sharma, M. G., Antle, C. E., & Button, J. (1994). *Binder characterization and evaluation* (SHRP A-369 Vol 3, Physical Characterization). Washington, DC: Strategic Highway Research Program, National Research Council.

Anderson, D. A., & Marasteanu, M. O. (1999). *Physical aging of asphalt binders relative to their glass transition temperature*. Transportation Research Board annual meeting, Washington, DC.

Anderson, D. A., Marasteanu, M. O., & Liu, Y. (1999). *Dilatometric measurements of glass transition temperatures*. Luxembourg: Eurobitume Workshop.

Baaj, H., Ech, M., Tapsoba, N., Sauzéat, C., & Di Benedetto, H. (2013). Thermomechanical characterisation of asphalt mixtures modified with high content of asphalt shingle modifier (ASM®) and reclaimed asphalt pavement (RAP). *Materials and Structures*, *46*(10), 1747–1763. doi:10.1617/s11527-013-0015-7

Bahia, H. U. (1991). *Low-temperature isothermal physical hardening of asphalt cements* (doctoral dissertation). Pennsylvania State University, University Park, PA.

Cannone Falchetto, A., Marasteanu, M. O., Balmurugan, S., & Negulescu, I. I. (2014). Investigation of asphalt mixture strength at low temperatures with the bending beam rheometer. *Road Materials and Pavement Design*, *15*(1), 28–44. doi:10.1080/14680629.2014.926618

Cannone Falchetto, A., Marasteanu, M. O., & Di Benedetto, H. (2011). Analogical based approach to forward and inverse problems for asphalt materials characterization at low temperatures. *Journal of the Association of Asphalt Paving Technologists*, *80*, 549–581.

Claudy, P., Letoffe, J. M., King, G., & Plancke, J. P. (1992). Characterization of asphalt cements by thermomicroscopy and differential scanning calorimetry: Correlation to classic physical properties. *Fuel Science and Technology International*, *10*(4–6), 735–765. doi:10.1080/08843759208916019

Delaporte, B., Di Benedetto, H., Chaverot, P., & Gauthier, G. (2009). Linear viscoelastic properties of bituminous materials including new products made with ultrafine particles. *Road Materials and Pavement Design*, *10*(1), 7–38. doi:10.1080/14680629.2009.9690180

Di Benedetto, H., Delaporte, B., & Sauzéat, C. (2007). Three-dimensional linear behaviour of bituminous materials: Experiments and modeling. *ASCE International Journal of Geomechanics*, *7*(2), 149–157. doi:10.1061/(ASCE)1532-3641(2007)7:2(149)

Di Benedetto, H., Neifar, M., Sauzéat, C., & Olard, F. (2007). Three-dimensional thermo-viscoplastic behaviour of bituminous materials: The DBN model. *Road Materials and Pavement Design*, *8*(2), 285–316. doi:10.1080/14680629.2007.9690076

Di Benedetto, H., Nguyen, Q. T., & Sauzéat, C. (2011). Nonlinearity, heating, fatigue and thixotropy during cyclic loading of asphalt mixtures. *Road Materials and Pavement Design*, *12*(1), 129–158. doi:10.3166/RMPD.12.129-158

Di Benedetto, H., & Olard, F. (2009). DBN law for the thermo-visco-elasto-plastic behaviour of asphalt concrete. In Y. Richard Kim (Ed.), *Modeling of asphalt concrete (pp. 245–263)*. New York, NY: ASCE Press, Mc Graw-Hill Construction.

Di Benedetto, H., Olard, F., Sauzéat, C., & Delaporte, B. (2004). Linear viscoelastic behaviour of bituminous materials: From binders to mixtures. *Road Material and Pavements Design*, *5*(S1), 163–202. doi:10.1080/14680629.2004.9689992

Di Benedetto, H., Sauzéat, C., & Sohm, J. (2009). Stiffness of bituminous mixtures using ultrasonic wave propagation. *Road Materials and Pavement Design*, *10*(4), 789–814. doi:10.1080/14680629.2009.9690227

EN 1426. (2007). *Bitumen and bituminous binders – determination of needle penetration*. Brussels: European Committee for Standardization.

EN 1427. (2007). *Bitumen and bituminous binders – determination of the softening point - Ring and ball method*. Brussels: European Committee for Standardization.

EN 14770. (2012). *Bitumen and bituminous binders – determination of complex shear modulus and phase angle – Dynamic shear rheometer (DSR)*. Brussels: European Committee for Standardization.

EN 14771. (2012). *Bitumen and bituminous binders – determination of the flexural creep stiffness - Bending beam rheometer (BBR)*. Brussels: European Committee for Standardization.

Farrar, M., Sui, C., Salmans, S., & Qin, Q. (2013). *Determining the low temperature rheological properties of asphalt binder using a dynamic shear rheometer (DSR)* (Product: FP 08). Laramie, WY: Fundamental Properties of Asphalts and Modified Asphalts, III, Western Research Institute.

Ferry, J. D. (1980). *Viscoelastic properties of polymers*. New York, NY: John Wiley.

Huet, C. (1963). *Etude par une méthode d'impédance du comportement viscoélastique des matériaux hydrocarbonés* (Doctoral dissertation). Faculté des sciences de Paris, Paris [in French].

Mangiafico, S., Di Benedetto, H., Sauzéat, C., Olard, F., Pouget, S., & Planque, L. (2013). Influence of RAP content on complex modulus of asphalt binder blends and corresponding mixes: Experimental results and modeling. *Road Materials and Pavement Design*, *14*(S1), 132–148. doi:10.1080/14680629.2013.774751

Mangiafico, S., Di Benedetto, H., Sauzéat, C., Olard, F., Pouget, S., & Planque, L. (2014). New method to obtain viscoelastic properties of bitumen blends from pure and reclaimed asphalt pavement binder constituents. *Road Materials and Pavement Design*, *15*(2), 312–329. doi:10.1080/14680629.2013.870639

Marasteanu, M. O., & Anderson, D. A. (2000). Comparison of moduli for asphalt binders obtained from different test devices. *Journal of the Association of Asphalt Paving Technologists*, *69*, 574–607.

Marasteanu, M. O., Cannone Falchetto, A., Turos, M., & Le, J-L. (2012). *Development of a simple test to determine the low temperature strength of asphalt mixtures and binders* (Report NCHRP IDEA 151). Washington, DC: Transportation Research Board.

Moon, K. H., Cannone Falchetto, A., & Marasteanu, M. O. (2013). Rheological modelling of asphalt materials properties at low temperatures: From time domain to frequency domain. *Road Materials and Pavement Design*, *14*(4), 810–830. doi:10.1080/14680629.2013.817351

Mounier, D., Di Benedetto, H., & Sauzéat, C. (2012). Determination of bituminous mixtures linear properties using ultrasonic wave propagation. *Construction and Building Materials*, *36*, 638–647. doi:10.1016/j.conbuildmat.2012.04.136

Neifar, M., & Di Benedetto, H. (2001). Thermo-viscoplastic law for bituminous mixtures. *Road Materials and Pavement Design*, *2*(1), 71–95. doi:10.1080/14680629.2001.9689894

Nguyen, H. M., Pouget, S., Di Benedetto, H., & Sauzéat, C. (2009). Time-temperature superposition principle for bituminous mixtures. *European Journal of Environmental and Civil Engineering*, *13*(9), 1095–1107. doi:10.3166/ejece.13.1095-1107

Nguyen, M. L., Sauzéat, C., Di Benedetto, H., & Tapsoba, N. (2013). Validation of the time–temperature superposition principle for crack propagation in bituminous mixtures. *Materials and Structures*, *46*(7), 1075–1087. doi:10.1617/s11527-012-9954-7

Nguyen, Q. T., Di Benedetto, H., & Sauzéat, C. (2012). Determination of thermal properties of asphalt mixtures as another output from cyclic tension-compression test. *Road Materials and Pavement Design*, *13*(N1), 85–103.

Nguyen, Q. T., Di Benedetto, H., Sauzéat, C., & Tapsoba, N. (2013). Time temperature superposition principle validation for bituminous mixes in the linear and nonlinear domains. *ASCE Journal of Materials in Civil Engineering*, *25*(9), 1181–1188. doi:10.1061/(ASCE)MT.1943-5533.0000658

Olard, F., & Di Benedetto, H. (2003). General 2S2P1D model and relation between the linear viscoelastic behaviors of bituminous binders and mixes. *Road Material and Pavement Design*, *4*(2), 185–224. doi:10.1080/14680629.2003.9689946

Olard, F., & Di Benedetto, H. (2005). The DBN model: A thermo-visco-elasto-plastic approach for pavement behavior modeling. Application to direct tension test and thermal stress restrained specimen test. *Journal of the Association of Asphalt Paving Technologists*, *74*, 791–827.

Pouget, S., Sauzéat, C., Di Benedetto, H., & Olard, F. (2010a). From the behaviour of constituent materials to the calculation and design of orthotropic steel bridge structures. *Road Materials and Pavement Design*, *11*(S1), 111–144. doi:10.1080/14680629.2010.9690329

Pouget, S., Sauzéat, C., Di Benedetto, H., & Olard, F. (2010b). Numerical simulation of the five-point bending test designed to study bituminous wearing courses on orthotropic steel bridge. *Materials and Structures*, *43*(3), 319–330. doi:10.1617/s11527-009-9491-1

Pouget, S., Sauzéat, C., Di Benedetto, H., & Olard, F. (2012). Modeling of viscous bituminous wearing course materials on orthotropic steel deck. *Materials and Structures*, *45*(7), 1115–1125. doi:10.1617/s11527–011–9820-z

Tapsoba, N., Sauzéat, C., Di Benedetto, H., Baaj, H., & Ech, M. (2014). Behavior of asphalt mixtures containing RAP and asphalt shingles. *Road Materials and Pavement Design*, *15*(2), 330–347. doi:10.1080/14680629.2013.871091

Tiouajni, S., Di Benedetto, H., Sauzéat, C., & Pouget, S. (2011). Approximation of linear viscoelastic model in the 3 dimensional case with mechanical analogues of finite size – Application to bituminous materials. *Road Materials and Pavement Design*, *12*(4), 897–930. doi:10.1080/14680629.2011.9713899